

Quantum Behavior in Mesoscale Lasers

A. F. J. Levi

University of Southern California, USA

Abstract— Describing the operation of mesoscale lasers consisting of several atom or semiconductor quantum dot emitters in an optical cavity is a challenge that, if properly addressed, may contribute to a new generation of efficient, ultra-small, photonic components. In dramatic contrast to successful continuum mean-field models of conventional macroscopic laser diodes, a quantum mechanical description of mesoscale lasers predicts steady-state and transient behavior that is dominated by fluctuations in the photon field and, in the limit of few emitters, the existence of symmetry-protected long-lived emitter states. Current understanding of these mesoscale laser phenomena suggests a very promising and challenging field for future study.

1. INTRODUCTION

To increase the number and type of applications for which semiconductor lasers may be used, it is natural to explore limits to reducing device size. Efficient and very small lasers might be useful for chip-scale optical interconnects in systems, displays, switches, sources of quantum light, and other applications. However, developing a realistic model that can simultaneously predict the behavior of conventional and small (*mesoscale*) lasers is a challenge as is the development of methods to control photon fluctuations in these devices.

2. SINGLE-MODE CONTINUUM MEAN-FIELD RATE EQUATIONS

The steady-state and transient average optical field intensity and average emitter excitation of a conventional macroscopic single-mode laser may be accurately described using continuum mean-field rate equations. The optical field of a macroscopic laser operating in the large particle number (thermodynamic) limit transitions from a disordered to an ordered state as the system is driven from below to above lasing threshold. This is *the* classical example of a second-order non-equilibrium phase transition with the optical field as the order parameter [1–6]. Mesoscale lasers are of interest in part because they must behave differently, if only because no formal non-equilibrium phase transition exists in a necessarily finite-sized meso-system.

Single-mode mean-field rate equations relating average injection current, I_{inj} , average light output, L_{out} , and average carrier density, n , have been used to predict some trends in device behavior as laser diode geometry is reduced in size. In particular, the phenomenological fraction of spontaneous emission, $0 < \beta \leq 1$, feeding into the laser mode can be used to parameterize laser diode scaling. To illustrate this, if it is assumed that the laser diode optical cavity may be reduced in size such that β increases but *no* other parameters change, Fig. 1 shows predicted (a) $L_{out} - I_{inj}$ and (b) $n - I_{inj}$ behavior on a log-log plot for the indicated values of β [7].

As may be seen in Fig. 1, the abrupt increase in light output with increasing current that is a conventional definition of laser threshold, I_{th} , becomes less well-defined as the device is reduced in size and β increases. When $\beta = 1$ all spontaneous emission feeds into the laser mode and there is no longer any evidence in the $L_{out} - I_{inj}$ characteristic of a definite transition from non-lasing to lasing. Similarly, carrier pinning above threshold disappears as β approaches unity. If the existence of a laser threshold implies a second-order nonequilibrium phase transition then, as β approaches unity, this transition is no longer well-defined in either the $L_{out} - I_{inj}$ or $n - I_{inj}$ behavior.

Other classical signatures of a nonequilibrium phase transition, such as critical slowing, are also suppressed as β is increased. In the case of critical slowing, a time delay t_d in the large-signal transient dynamics exists between the onset of a step change in diode forward current for time $t \geq 0$ from zero current at time $t < 0$ and laser light output L_{out} to reach half of the steady-state value.

Figure 2(a) plots calculated time delay, t_d , as a function of step current in the range $0 < I_{step} < 20$ mA for the indicated values of spontaneous emission factor β . There is an increase in delay for values of current near threshold current, $I_{th} = 5.7$ mA. Critical slowing is due to long-lived fluctuations associated with the existence of a phase transition [8]. Increasing the value of β damps the critical slowing phenomena and, for a given step increase in injection current, reduces the off-on time delay, t_d . However, this does *not* mean that a laser diode with $\beta \sim 1$ has a faster *small-signal*

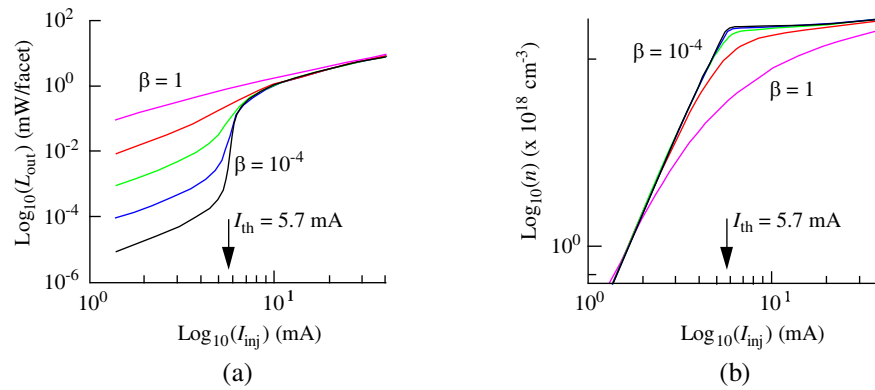


Figure 1. (a) Light emission and (b) carrier density in a Fabry-Perot laser diode for values of spontaneous emission factor $\beta = 10^{-4}$, $\beta = 10^{-3}$, $\beta = 10^{-2}$, $\beta = 10^{-1}$, and $\beta = 1$ plotted using logarithmic scales. The calculation uses typical parameters for an InGaAsP device with emission at 1310 nm wavelength.

on-on modulation response compared to a conventional device with $\beta \ll 1$. This is because as β becomes large carriers are no longer pinned and so the carrier recombination rate due to stimulated emission never dominates.

Figure 2(b) plots inverse delay time as function of current and shows that $1/t_d \propto I_{step}$ for current $I_{inj} > I_{th}$. The minimum value of the dip in $1/t_d$ at I_{th} is proportional to an energy gap that separates the sustained lasing and non-lasing states of the system.

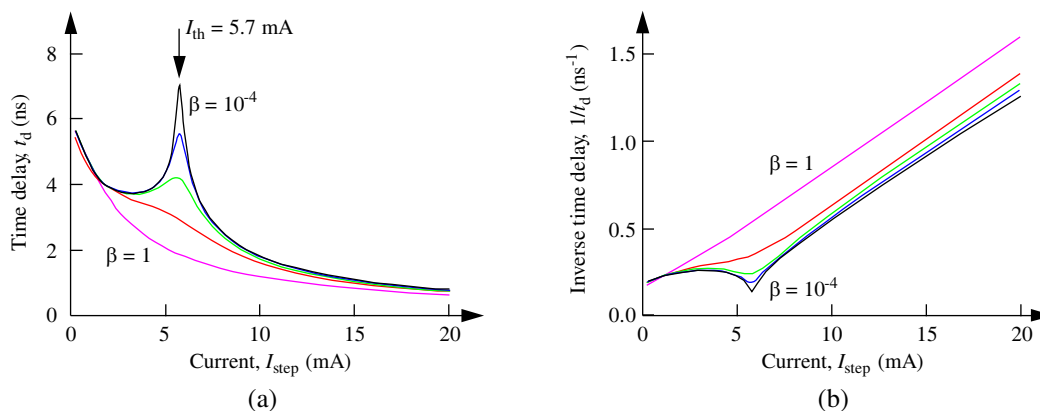


Figure 2. (a) Time delay, t_d , as a function of step current I_{step} for values of spontaneous emission factor $\beta = 10^{-4}$, $\beta = 10^{-3}$, $\beta = 10^{-2}$, $\beta = 10^{-1}$, and $\beta = 1$. (b) Inverse of time delay, $1/t_d$, as a function of step current for the same values of spontaneous emission factor, β , used in (a). The calculation uses the same parameters as in Fig. 1.

3. FLUCTUATIONS

The analogy between the statistical properties of laser light and second-order thermodynamic phase transitions has practical consequences. Lasing light is ordered and spontaneous emission is not. As injection current approaches the threshold current of a laser diode (LD) *unsustainable* fluctuations into a lasing state increasingly convert carriers into photons. These fluctuations contribute to below-threshold reduction in carrier density. Optical emission from a laser diode consists of lasing and nonlasing components. The nonlasing component has spectrally broadband emission into nonlasing optical modes, similar to that of a light emitting diode (LED). The lasing component has spectrally narrow-band emission into the lasing mode and temperature dependence below threshold that is well characterized by a power law, in direct analogy with Landau-Ginzburg theory of second-order phase transitions [9].

A Fabry-Perot laser diode (LD) can become a light emitting diode (LED) by anti-reflection coating the cavity mirrors of the device. In this way the influence of subthreshold fluctuations in a LD can be compared to a LED of the *same* geometry and active region [10, 11]. Experiments

suggest that subthreshold fluctuations into the laser cavity modes of a LD extract a current, I_{fl} , that is of increasing relative importance in determining threshold current as temperature increases.

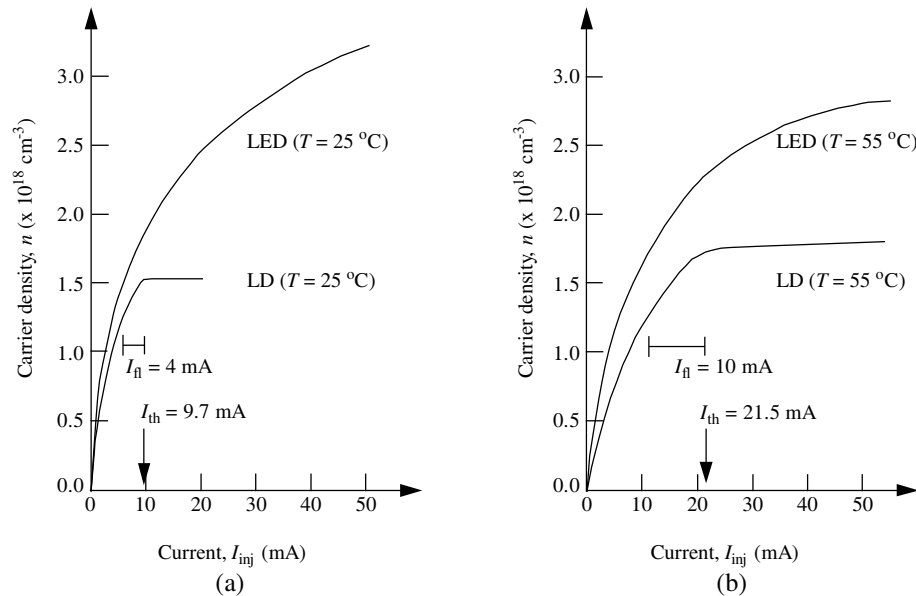


Figure 3. Carrier density, n , as a function of injection current, I_{inj} , for light emitting diode (LED) and laser diode (LD) of the same geometry and active region. (a) Temperature $T = 298\text{ K}$ (25°C), LD threshold current $I_{th} = 9.7\text{ mA}$, and $I_{fl} = 4\text{ mA}$. (b) Temperature $T = 328\text{ K}$ (55°C), LD threshold current $I_{th} = 21.5\text{ mA}$, and $I_{fl} = 10\text{ mA}$. Fluctuations enhance lasing emission below threshold and remove carriers below threshold. Fluctuations contribute to the temperature dependence of LD threshold current.

Figure 3 shows carrier density n versus injection current, I_{inj} , for LD and LED of the same geometry and active region measured at two different temperatures. Carrier density in the LED is a less nonlinear function of injection current and less sensitive to temperature than the LD. Photons fluctuating into cavity modes of the LD cause carrier density to be suppressed more effectively than in the corresponding LED device. Thus, to reach lasing threshold current, I_{th} , an *extra current*, I_{fl} , is required to overcome the effects of carrier suppression due to photon fluctuations. The current I_{fl} is the difference in drive current between LED and LD to reach LD threshold carrier density, n_{th} . Figure 3(a) shows that I_{fl} accounts for almost half the LD threshold current, I_{th} . At elevated temperatures the threshold carrier density increases, fluctuations are enhanced, and the contribution of I_{fl} increases. Subthreshold fluctuations act as a feedback mechanism that cause laser threshold current I_{th} to increase with increasing temperature.

4. SEMICLASSICAL MASTER EQUATIONS

As a first step to capture the physics dominating mesoscale laser behavior, semiclassical master equations with continuum probability functions to describe quantized particle number states may be used. This approach reveals that quantum fluctuations dominate steady-state and transient response in small devices [12, 13]. The fluctuations and the fact that a lowest energy state of the system exists, suppress lasing and enhance spontaneous emission near threshold, and create non-Poisson probability distributions for excited electronic states and photon number. However, while the semiclassical master equations account for energy and particle number conservation they do not include phase fluctuations and important correlation effects. In particular, they cannot be used to predict the existence of symmetry-protected entangled quantum dark states.

5. QUANTUM MODEL

A laser requires at least one externally driven emitter interacting with a photon mode of a cavity. Practical devices consist of multiple atoms (or semiconductor quantum dots) in an optical cavity. The emitters are driven by an external reservoir such as a battery in the case of a semiconductor device. Rather than specify a laser diode current, the emitters of a mesoscale laser may be considered to be driven by a more general pump that excites emitters at a rate P . Photons generated by

deexcitation of emitter electron states are coupled via partially reflecting mirrors of the cavity to external continuum reservoir modes. A mesoscale laser can be modeled as consisting of a positive non-zero integer number, N_e , two-level atom or quantum dot emitters incoherently pumped by an external reservoir and interacting with a quantized photon field that has a positive integer number, S_{num} , cavity photons that can decay into an external reservoir through finite reflectivity mirrors.

In a fully quantum model of a single quantum dot laser [14] or mesoscale laser [15], the Hamiltonian describing N_e two-level emitters is

$$H = H_S + H_R + H_{RS} \quad (1)$$

where H_S is the Hamiltonian of the system of emitters and cavity photons, H_R is the Hamiltonian for the reservoirs, and H_{RS} couples the system to the reservoirs. For a homogeneous system of identical emitters, H_S is often taken to be the Jaynes-Cummings Hamiltonian [16] coupling a single-cavity mode with a sum over the N_e two-level emitters. The emitter electronic states are continuously incoherently pumped at rate P by an external reservoir. The stimulated and spontaneous emission coefficient coupling the ground $|1\rangle$ and excited $|2\rangle$ electronic states of each emitter is g . The separation in emitter eigenenergy is $\hbar\omega = E_2 - E_1$, where, on resonance, ω is the angular frequency of the high-Q optical cavity resonance. The emitters are damped at rate γ by a reservoir of oscillators representing incoherent decay via spontaneous emission into nonlasing leaky modes. Decay of the laser photon field in the single-cavity mode is by coupling to another external reservoir through partially transmitting mirrors with total photon loss rate κ . To emphasize the role of quantum fluctuations in determining behavior, the system is assumed to be maintained at zero absolute temperature.

Figure 4 shows results of calculating steady-state properties for the indicated number of two-level emitters coupled to a single-mode cavity field as a function of incoherent *normalized* pump rate P_{norm} using a \log_{10} scale ($P_{norm} = P/N_e$, the pump rate divided by the number of emitters). In the Figure, (a) is the average photon number $\langle S_{num} \rangle$ in the lasing mode, (b) is net average inversion of emitters $\langle \sigma_2 - \sigma_1 \rangle$, (c) is the Fano-factor (relative variance) of photon fluctuations, $(\langle S_{num}^2 \rangle - \langle S_{num} \rangle^2) / \langle S_{num} \rangle = \sigma_{S_{num}}^2 / \langle S_{num} \rangle$, and (d) is the time-averaged spectral linewidth $\Delta\omega_{FWHM}$ of photon emission into the laser mode. Unlike a macroscopic device, there is no abrupt change in slope of $\langle S_{num} \rangle$ with increasing pump that can be associated with laser threshold pump value, P_{th} . For this reason, the laser threshold of a mesoscale laser is taken to occur at the peak in photon Fano-factor at low pump rate (in this case when $P_{norm} < 1$ meV). High pump levels cause emitter inversion to saturate and a corresponding *self-quenching* peak in average photon number $\langle S_{num} \rangle$ occurs (in this case when $P_{norm} > 10$ meV). The pump value at which the associated peak in photon Fano-factor occurs is P_{sq} . Calculated behavior shown in Fig. 4 is for $1 \leq N_e \leq 5$.

Initially, full-width-at-half-maximum spectral line width, $\Delta\omega_{FWHM}$, decreases with increasing pump rate. However, self-quenching causes a peak in $\langle S_{num} \rangle$ and fluctuations in photon number, as measured by Fano factor $\sigma_{S_{num}}^2 / \langle S_{num} \rangle$, also peaks near these pump levels due to dissipation associated with self-quenching. The same mechanism increases the photon emission spectral line width, $\Delta\omega_{FWHM}$.

Mesoscale lasers are not lasers in the sense usually associated with macroscopic devices. Conventional semiconductor laser diodes contain many emitters and when driven near threshold can be characterized by a well-defined nonequilibrium phase transition in which the photon field is the order-parameter. While such a phase transition formally only exists in the thermodynamic limit, mesoscale lasers retain signatures of lasing in conventional macroscopic devices such as inversion pinning and a peak in photon fluctuations near pump threshold. Reducing photon losses by decreasing κ and γ , and enhancing total optical gain by increasing N_e , scales meso-laser characteristics towards classical, and hence demonstrably useful, behavior. However, in very small devices, self-quenching associated with a low value of N_e limits performance at high pump rates. Self-quenching is a fundamentally finite-size effect associated with meso-scale lasers.

As a direct consequence of the fluctuation-dissipation theorem [17], both self-quenching and laser threshold are associated with peaks in photon Fano-factor. At low values of pump there can also exist special symmetry-protected entangled quantum states [18]. A well-known example occurs when $N_e = 2$ and each emitter has identical coupling strength g . The symmetry of the entangled two-emitter singlet state is such that photon emission into the cavity mode is not allowed, resulting in a long-lived (almost) dark state. However, as shown in Fig. 5, with increasing pump, dissipation and an associated peak in photon emission Fano-factor occurs at pump value P_{sym} as dark-state

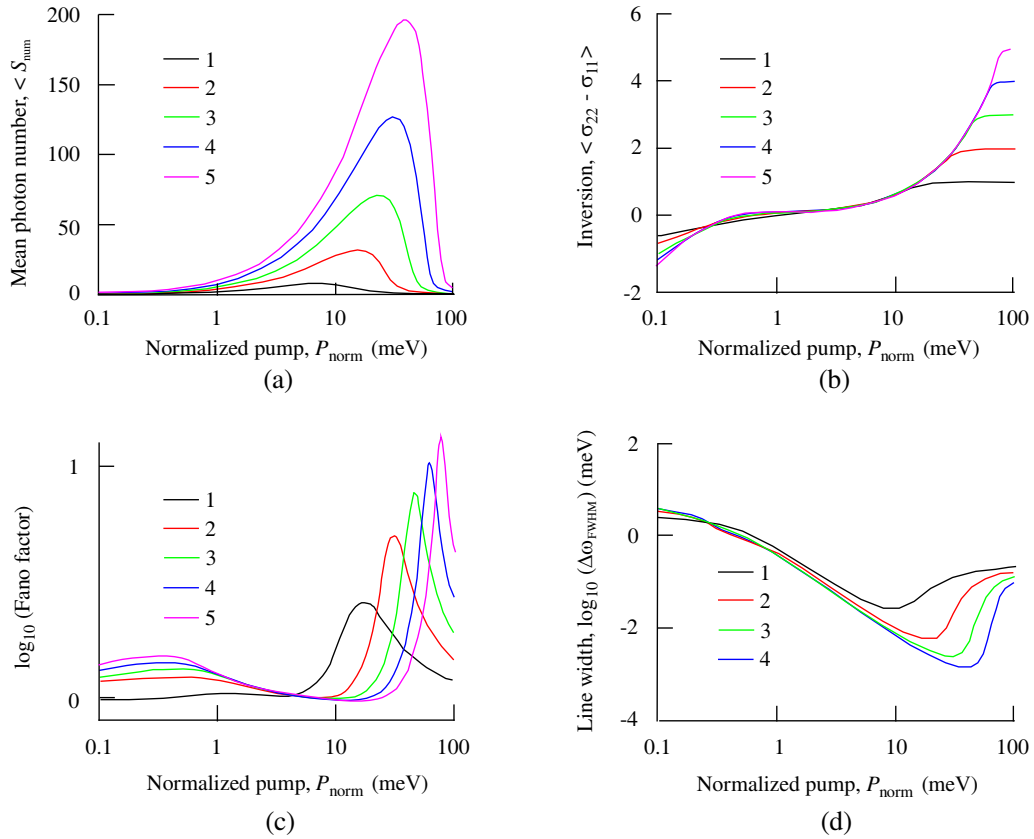


Figure 4. Calculated steady-state properties for the indicated number of two-level emitters coupled to a cavity field with normalized incoherent pump P_{norm} . (a) Mean photon number in lasing mode. (b) Average net inversion of emitters. (c) Photon Fano-factor. (d) Spectral line width. Laser threshold corresponds to Fano-factor peak with $P < 1$ meV. The Fano-factor peak due to self-quenching occurs when $P > 10$ meV. The horizontal axis shows the pump value divided by number of emitters and is plotted using a \log_{10} scale. Behavior for different number of emitters is shown with $N_e = 1$ (black), $N_e = 2$ (red), $N_e = 3$ (green), $N_e = 4$ (blue), and $N_e = 5$ (magenta). Parameters are: $g = 1$ meV; $\gamma = 0.1$ meV; $\hbar\omega = 1000$ meV; $\kappa = 0.25$ meV.

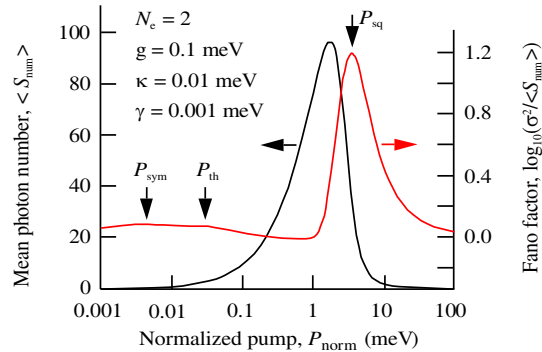


Figure 5. Calculated steady-state mean photon number and photon Fano-factor for $N_e = 2$ two-level emitters coupled to a cavity field with incoherent pump P_{norm} . Laser threshold corresponds to broad peak in Fano factor at pump value P_{th} . Peak due to self-quenching occurs at pump value P_{sq} . The peak in photon Fano-factor at pump value P_{sym} occurs due to dissipation associated with the destruction of the symmetry-protected state. Parameters g , κ , and γ are indicated.

lifetime is reduced. This photon Fano-factor peak is an experimentally measurable indicator of where, as a function of pump, the system transitions between different operational characteristics [19]. In general, the boundary region between different modes of operation is associated with dissipation and hence fluctuations. Dissipation occurs because the lifetime of states necessarily changes as the system transitions between different modes of operation. For $P < P_{sym}$ the device

behavior is dominated by the presence of long-lived dark-states. For pump values $P_{sym} < P < P_{th}$ spontaneous emission and sub-threshold fluctuations occur, and for pump values $P_{th} < P < P_{sq}$ average net inversion of emitters is pinned and lasing dominates. When pump values $P > P_{sq}$ emitter inversion in the finite-sized system saturates, self-quenching occurs, and there is a peak in photon fluctuations.

6. CONCLUSION

Photon fluctuations in both classical macroscopic and mesoscale lasers play an important role in determining device performance. Control of fluctuations can result in useful device behavior. For example, a macroscopic laser diode operating close to the thermodynamic limit can have a lasing mode emission linewidth and photon Fano-factor that decreases with increasing injection current $I_{inj} > I_{th}$. In contrast, the reduction in linewidth and reduction in photon Fano-factor in a meso-laser as pump is increased to values greater than P_{th} is limited by the existence of self-quenching as pump values approach P_{sq} . Overcoming such practical limitations associated with mesoscale lasers presents an interesting challenge whose successful solution might be demonstrated by showing control of fluctuations caused by laser threshold, self-quenching, or dissipation in symmetry-protected quantum states.

REFERENCES

1. De Giorgio, V. and M. O. Scully, “Analogy between the laser threshold region and a second-order phase transition,” *Phys. Rev. A*, Vol. 2, No. 4, 1170–1177, 1970.
2. Graham, R. and H. Haken, “Laserlight — first example of a second-order phase transition far away from thermal equilibrium,” *Z. Physik.*, Vol. 237, No. 1, 31–46, 1970.
3. Grossmann, S. and P. H. Richter, “Laser threshold and nonlinear Landau fluctuation theory of phase transitions,” *Z. Physik.*, Vol. 242, No. 5, 458–475, 1971.
4. Corti, M. and V. Degiorgio, “Analogy between the laser and second-order phase transitions: Measurement of “coexistence curve” and “susceptibility” for a single-mode laser near threshold,” *Phys. Rev. Lett.*, Vol. 36, No. 20, 1173–1176, 1976.
5. Pakhalov, V. B. and A. S. Chirkin, “Phase transitions in formation of spatially coherent laser beams,” *Sov. J. Quantum Electron.*, Vol. 7, No. 6, 715–719, 1977.
6. Salomaa, R. and S. Stenholm, “Observable manifestations of phase transitions in lasers,” *Appl. Phys.*, Vol. 14, No. 4, 355–360, 1977.
7. Levi, A. F. J., “Essential semiconductor laser device physics,” Morgan and Claypool, San Rafael, California, 2018.
8. Haken, H., “Cooperative phenomena in systems far from thermal equilibrium and in nonphysical systems,” *Rev. Mod. Phys.*, Vol. 47, No. 1, 67–121, 1975.
9. O’Gorman, J., A. F. J. Levi, S. Schmitt-Rink, T. Tanbun-Ek, D. L. Coblenz, and R. A. Logan, “On the temperature sensitivity of semiconductor lasers,” *Appl. Phys. Lett.*, Vol. 60, No. 2, 157–159, 1992.
10. Chuang, S. L., J. O’Gorman, and A. F. J. Levi, “Amplified spontaneous emission and carrier pinning in laser diodes,” *IEEE J. Quantum Electron.*, Vol. 29, No. 6, 1631–1639, 1993.
11. O’Gorman, J., S. L. Chuang, and A. F. J. Levi, “Carrier pinning by mode fluctuations in laser diodes,” *Appl. Phys. Lett.*, Vol. 62, No. 13, 1454–1456, 1993.
12. Roy-Choudhury, K., S. Haas, and A. F. J. Levi, “Quantum fluctuations in small lasers,” *Phys. Rev. Lett.*, Vol. 102, No. 5, 053902(1–4), 2009.
13. Roy-Choudhury, K. and A. F. J. Levi, “Quantum fluctuations in very small laser diodes,” *Phys. Rev. A*, Vol. 81, No. 1, 013827(1–11), 2010.
14. Perea, J. I., D. Porras, and C. Tejedor, “Dynamics of the excitations of a quantum dot in a microcavity,” *Phys. Rev. B*, Vol. 70, No. 11, 115304(1–13), 2004.
15. Roy-Choudhury, K. and A. F. J. Levi, “Quantum fluctuations and saturable absorption in mesoscale lasers,” *Phys. Rev. A*, Vol. 83, No. 4, 043827(1–9), 2011.
16. Jaynes, E. T. and F. W. Cummings, “Comparison of quantum and semiclassical radiation theories with application to the beam maser,” *Proc. IEEE*, Vol. 51, No. 1, 89–109, 1963.
17. Kubo, R., “The fluctuation-dissipation theorem,” *Rep. Prog. Phys.*, Vol. 29, 255–284, 1966.
18. Zanardi, P., “Dissipative dynamics in a quantum register,” *Phys. Rev. A*, Vol. 56, No. 6, 4445–4451, 1997.
19. Abouzaid, A., W. Unglaub, and A. F. J. Levi, “Long-lived entangled emitter states in meso-lasers,” unpublished.